ENCIT 2018

ABCM Associação Brasileira de Engenharia e Ciências Mecânicas

17th Brazilian Congress of Thermal Sciences and Engineering
November 25th-28th, 2018, Águas de Lindóia, SP, Brazil

ENCIT-2018-0081
NUMERICAL ANALYSIS OF LAMINAR MIXED CONVECTION FROM A ROTATING CYLINDER IN CROSS FLOW

Ariane Neale Ramos Vieira
arianealev@gmail.com

Ana Lúcia Fernandes de Lima E Silva
Sandro Metrevelle Marcondes de Lima E Silva
Federal University of Itajubá - UNIFEI, Institute of Mechanical Engineering - IEM, Prof. José Rodrigues Seabra Campus, 1303 BPS Av., Pinheirinho District, ZIP code 37500-903, Box-Postal 50, Itajubá, Minas Gerais, Brazil.
alfsilva@unifei.edu.br
metrevel@unifei.edu.br

Abstract. *Numerical simulations were performed to analyze mixed convection around a stationary/rotating heated cylinder in cross flow. Cases configuration include different values of Reynolds ($40 \leq Re \leq 200$) and Richardson ($0.5 \leq Ri \leq 2$) numbers and different specific rotations ($0 \leq \alpha \leq 2$). A set of simulations were performed with a home-made programbased on the Immersed Boundary Method (IBM) with the Virtual Physical Method (VPM). Another set of simulations were performed using the open source program OpenFOAM. The vortex shedding patterns and pressurefields are presented and different aspects due to the different specific rotation values are discussed. The results were compared with the literature and demonstrated good agreement between them. Time averaged values of drag and lift coefficients, as well as Strouhal and Nusselt numbers were analyzed. It was proposed an empirical correlation for the Nusselt number, as a function of Reynolds number and specific rotation using the obtained results. This correlation demonstrate good agreement with the simulated data and the expected physical behavior of this type of flow reported on literature.*

Keywords: *Mixed Convection, Rotating Circular Cylinder, Immersed Boundary Method/Virtual Physical Method, OpenFOAM.*

1. INTRODUCTION

Heat transfer through convection is broadly present in different types of thermal systems, such as power plant generation, domestic and industrial heating, ventilation and air conditioning equipment, in the pipeline transport of different fluids, in certain types of industrial process (for example, heated rollers of pulp and paper industry), or yet, in the cooling process of electronic devices, among other applications. Thus, convection has been largely studied for a great variaty of scenarios that involve confined/external flows and different hydraulic diameters and geometries. However, most of them have dealt with forced convection. In the past years the aim was placed into increasing efficiency of engineerging systems, as much as there were a growth of heat loads and systems dimensions in technological applications. Therefore, forced convection simplification is no longer possible to be made in certain cases, in such a way mixed convection analysis is required for those systems.

Furthermore, as the problem of stationary bodies has a considerable number of published work, problems in which there are moving heated boundaries are more uncommon on literature. Geometry motion can be caused by mechanical vibration phenomenon or can even be intrinsic to the process (as the case of heated rollers). The interaction of the flow due to the geometry boundary motion and the flow due to the buoyancy effect produce a complex flow dynamics. A comprehensive analysis is needed to understand the physics of the resulting flow and the heat transfer process. Different configurations and combinations of thermal and dynamical boundary conditions have been considered and analysed. For this work only external flows were considered, more specificaly, it was studied the mixed convection due to fluid flow around a circular heated cylinder in a cross flow configuration (in which the buoyancy effects are perpendicular to the incident flow). The physics behind this type of flow has been already studied by a few authors and a small summary is presented below.

Badr (1983) analytically studied the mixed convection around a stationary heated cylinder for Reynolds values between 1 and 40 and cross flow. Grashof values were ranged from 0 to 6400 ($0 \leq$ Ri = $Gr/Re^2 \leq 4$) and the Prandtl number was set constant at 0.7. The analytical results were compared with experimental results and showed good agreement. The temporal and spatial behavior of streamlines and isotherms around the cylinder was analyzed and the influence of buoyancy indicates an increase in the heat transfer process, as there is a growth of Nusselt number.

Kieft, Rindt and van Steenhoven (2007) studied the mechanism of vortex detachment of a flow around a heated stationary circular cylinder in cross flow with a high order spectral element method (SEM). The simulations were performed for a constant Reynolds number of 75, Prandlt number of 0.7 and Richardson numbers between 0 and 1. The process of formation and evolution of vortices was analyzed. Temperature distribution along the cylinder surface were presented with isotherms at specific times. The authors concluded that due to the heating of the fluid, there is a process of imbalance of forces, leading to an asymmetry in the downstream of the vortex street.

Bhattacharyya and Singh (2010) numerically studied the process of vortex formation around a stationary circular cylinder subjected to a cross flow for Reynolds numbers between 50 and 200 and Richardson numbers between 0 and 2. They used a pressure correction based on the iterative algorithm SIMPLE (Semi-Implicit Method for Pressure Linked Equations) implemented in a particular code. The role of buoyant effects in the induction of baroclinic vorticity and vortex wake was studied. The mean values of Nusselt numbers and drag and lift coefficients were calculated for all simulations and their temporal evolution were analyzed for some of the cases studied. The flow pattern found for those cases were asymmetric and with negative values of lift coefficients. The authors stated that it occurs because as the fluid near the cylinder is heated, it rises due to the specific mass variation, thus the final velocity at the bottom of the cylinder is greater than the velocity at the top. According to them, as a result of this velocity imbalance the cylinder experience a net negative lifting force.

Paramane and Sharma (2010) used a particular code with a semi-explicit finite-volume method to study the combined effects of mixed convection associated with the rotation of heated cylinders for cross flows. They simulated cases with Reynolds numbers of 40 and 100, specific rotation between 0 and 8, constant Prandtl number of 0.7 and Richardson numbers equal to 0 (forced convection), 0.5 and 1 (mixed convection cases). They found that for critical values of rotation, each one given for a specific pair of Reynolds and Richardson numbers, vortex shedding is suppressed. They kept increasing even more the rotation after that supression and observed that a new frequency of vortex detachment appears. These new vortex formation had a lower value of frequency, compared to the initially value registered for lower rotation. The temporal evolution, as well as the average values for the lift and drag coefficients and Nusselt numbers were analyzed. The authors showed through these coefficients that the rotation can be used to reduce drag and decrease heat transfer.

Santos (2014) studied the forced convection flow around a heated circular cylinder considering stationary and rotating cases. The author used the Immersed Boundary Method with the Virtual Physical Model (IBM-VPM) implemented in a home-made program written in C ++ language. This methodology was first proposed by Lima E Silva (2002) and was very succesfully tested for different cases, such as: Lima E Silva, Silveira-Neto and Damasceno (2003) simulated flows over a circular cylinder, Vilaça, Lima E Silva and Silveira-Neto (2004) adapted the method for the case of a fluid flow around a free falling particle, Oliveira, Lima E Silva and Silveira-Neto (2006) simulated turbulent flows around airfoils, and Lima E Silva, Silva and Silveira-Neto (2007) studied complex flows around bluff bodies. Also, Lima E Silva and Lima E Silva (2007) succesfully studied buoyancy-driven flows over a square cylinder using the IBM-VPM. Santos (2014) analyzed the dynamics of the fluid flow due to the thermal field in association with different specific rotations of the cylinder. Several simulations were performed and the drag, lift and pressure coefficients were evaluated, as well as the Strouhal and Nusselt numbers. The author also analyzed the velocity, pressure, vorticity and temperature fields through streamlines and isoterms and compared his results with those of the literature.

Chatterjee and Sinha (2016) used the commercial CFD package Ansys Fluent to study the vortex detachment phenomenon in the wake of a heated cylinder for different values of Prandtl number and specific rotation. The simulations covered Prandtl numbers of 0.71, 7 and 100, Richardson numbers between 0 and 2, and a fixed Reynolds number of 40. Specific rotations varied from 0 to 4. They also observed that from a critical value of Richardson number, vortex detachment phenomenon occurs, even for the subcritical Reynolds number of 40. The authors proposed an approach based on the Stuart-Landau extended model to estimate the critical value of Richardson number, from which there is vortex formation. They observed that, due to the stabilization effect of the Prandtl number, the critical Richardson numbers necessary to destabilize the flow increases with the Prandtl number. They also observed that the rotation had a similar stabilizing effect as it increased the value of critical Richardson number for each simulated case. As previous observed by Paramane and Sharma (2010), they noticed that rotation reduces the heat transfer exchange and their simulations showed lower mean Nusselt numbers with the increase of the specific rotation.

In the present work two different numerical methodologies were used to study the cross flow around a heated circular cylinder. Stationary and rotating cases were simulated for mixed convection cases with different Reynolds and Richardson numbers.

2. MATHEMATICAL AND NUMERICAL FORMULATION

The schematic representation of the spatial domain of the studied problem with its boundary conditions are shown in Fig. 1. The top and bottom sides of the domain are treated as slip boundaries to emulate unconstrained flow. Fluid enters through the left side with a constant temperature θ_f, with constant velocity u in accordance with the defined Reynolds number. The outlet boundary conditions are null gradient of velocity and pressure imposed, which means no jet is formed.

Gravitational effect is set to be at the y axis downward to characterize a cross flow. All simulations were carried out with a computational domain of length $L = 60D$ and height of $H = 50D$, where D is the cylinder diameter. The circular cylinder was set at a $20D$ distance from the inlet and at the middle of the domain, $30D$ of height. Also, the cylinder was considered a no-slip boundary (for OpenFOAM only) with a constant temperature, $\theta_c > \theta_f$ (heated surface), and with a specific rotation, α, the ratio of the rotation speed of the cylinder, V, and the incident velocity, u.

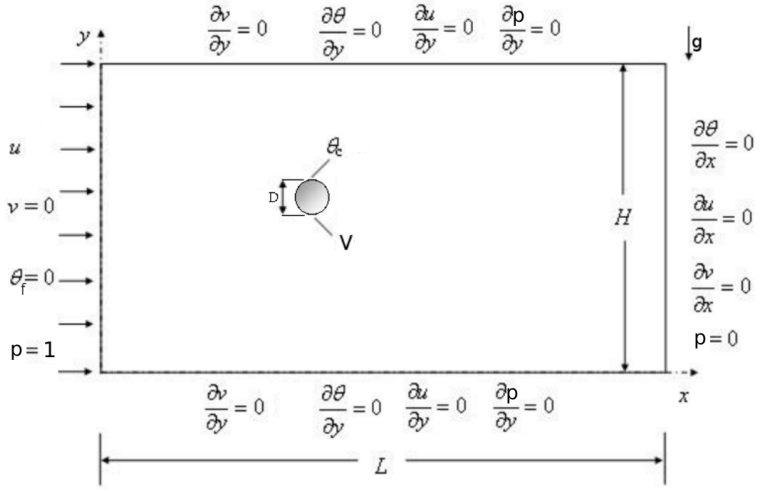

Figure 1: Two-dimensional domain with its boundary conditions.

The fluid was considered newtonian and incompressible. Boussinesq approximation was assumed for the buoyancy effect. No heat generation was taken into account as well as no rotation of the coordinate system. The governing equations of the continuity, momentum and energy were written and implemented for the IBM-VPM in a non-dimensional form. For the OpenFOAM software were used the same dimensionless parameters of the IBM-VPM cases.

2.1 The Immersed Boundary Method/Virtual Physical Model

In the IBM-VPM a mixed eulerian-lagrangian formulation is used to represent the flow and the immersed boundary. A cartesian non-uniform grid was used to describe the flow with a finite difference method for the discretization. The cylinder geometry is represented by a lagrangian grid with a uniformly distributed finite number of points. The eulerian and the lagrangian grids were coupled by force and heat fields calculated iterativaly for each lagrangian point and then distributed to the eulerian nodes in the body neighborhood. The continuity, momentum and energy non-dimensional equations can be written as:

$$\frac{\partial u}{\partial x} + \frac{\partial v}{\partial y} = 0 \tag{1}$$

$$\frac{\partial u}{\partial t} + u\frac{\partial u}{\partial x} + v\frac{\partial u}{\partial y} = -\frac{\partial p}{\partial x} + \frac{1}{Re}\nabla^2 u + Ri\theta + f_x \tag{2}$$

$$\frac{\partial v}{\partial t} + u\frac{\partial v}{\partial x} + v\frac{\partial v}{\partial y} = -\frac{\partial p}{\partial y} + \frac{1}{Re}\nabla^2 v + f_y \tag{3}$$

$$\frac{\partial \theta}{\partial t} + u\frac{\partial \theta}{\partial x} + v\frac{\partial \theta}{\partial y} = \frac{1}{RePr}\nabla^2 \theta + q \tag{4}$$

As it can be noticed, the Dirichlet boundary conditions of velocity and temperature on the surface of the cylinder are indirectly imposed through the force ($\vec{f}$) and energy (q) terms added to the governing equations. These terms model the immersed body and can be calculated by:

$$\vec{f}(\vec{x_i}, t) = \sum \vec{F}(\vec{x_k}, t) D_{i,j}(\vec{x_k})(\vec{x_i} - \vec{x_k})\Delta s^2 \tag{5}$$

$$q(\vec{x_i}, t) = \sum Q(\vec{x_k}, t) D_{i,j}(\vec{x_k})(\vec{x_i} - \vec{x_k})\Delta s^2 \tag{6}$$

where F and Q are calculated through the temperature, velocity and pressure values, interpolated from the eulerian grid. $D_{i,j}$ is a gaussian distribution function and Δs is the distance between two lagrangian points. The Virtual Physical Model

proposed by Lima E Silva (2002) is used to obtain the lagrangian quantities, over the immersed boundary, through the following equations:

$$\vec{F}(\vec{x},t) = \frac{\partial \vec{U}}{\partial t} + (\vec{U}\cdot\vec{\nabla})\vec{U} - \frac{1}{Re}\nabla^2\vec{U} + \vec{\nabla}p \tag{7}$$

$$Q(\vec{x},t) = \frac{\partial \theta}{\partial t} + \vec{U}\cdot\vec{\nabla}\theta - \frac{1}{RePr}\nabla^2\theta \tag{8}$$

The governing quations were discretized with a second order finite difference in space and the second order Runge-Kutta method for time. The coupling between pressure and velocity was done with a Fractional Step method based on a pressure correction scheme. More details can be seen in Lima E Silva (2002). Inside the cylinder was used a uniform mesh with a minimum of 80 eulerian grids for all simulations. This value was set after refinement studies from previous works. The final mesh, eulerian and lagrangian can be seen on Fig. 2.

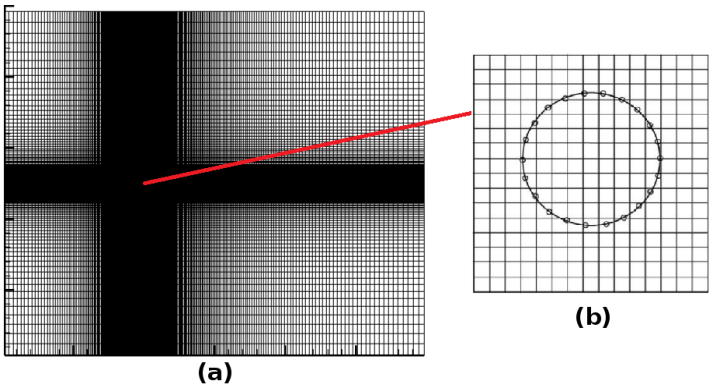

Figure 2: IBM-VPM mesh used for all simulations. **(a)** Eulerian mesh. **(b)** Zoom view of the cylinder.

2.2 OpenFOAM program

OpenFOAM is an open-source software written in C++ based on the Finite Volume method. The program has different tools for meshing, solving and pos-processing applied for CFD analysis, including buoyant flows. For this work, version 4.0 was used to solve the governing equations through the *buoyantBoussinesqPimpleFoam* solver. This solver uses a PIMPLE algorithm, which consists of a combination of the PISO algorithm (pressure-implicit with splitting of operators) applied for the pressure-velocity coupling with an adapted version of the SIMPLE algorithm (Semi Implicit Method for Pressure Linked Equations) to model the density variation through Boussinesq approximation.

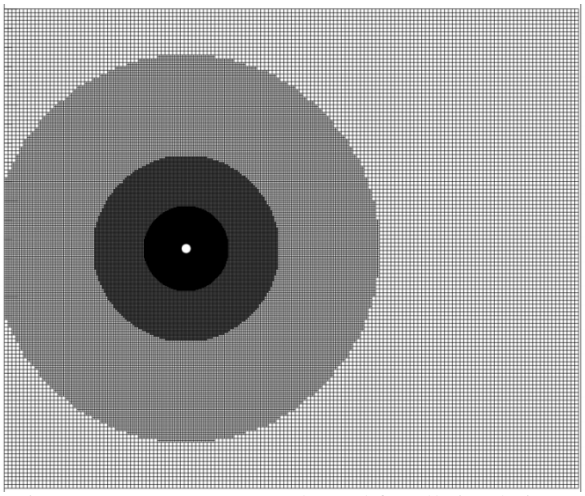

Figure 3: OpenFOAM mesh used for all simulations.

A first order Euler discretization was used for the local time derivative and the gradient term is reconstructed by the Gauss linear method. A second-order upwind scheme was used to deal with the convective terms, and the second-order Gauss-linear approach to handle the diffusion terms. The mesh was generated using the *snappyHexMesh* tool. This technique is able to automatically generate meshes, iteratively refining a starting cartesian mesh, from triangulated surface

geometries in Stereolithography (STL) or Wavefront Object (OBJ) formats. An ilustration of the mesh can be seen on Fig. 3, which was used for the simulations performed with this program.

The Conjugate Gradient method was used to solve the linear systems for pressure and the Conjugate Gradient method with preconditioning was used to solve the linear systems of velocity and temperature. The under-relaxation factors for all equations were set to 0.7, and the threshold of residuals, which is defined based on the infinity norm for each time-step, were equal to 10^{-6}.

3. RESULTS AND DISCUSSIONS

All simulations were performed for a fixed Prandtl number of 0.7, with Reynolds and Richardson numbers and specific rotation varying according to Tab. 1. In the IBM-VPM program a unit constant was used for the dimensionless temperature of the cylinder, $\theta_c = 1$, and a zero constant for the fluid, $\theta_f = 0$. In the simulations with OpenFOAM, the cylinder temperature was set to a constant value of $\theta_c = 302K$ and the inlet temperature as well as the entire domain initial temperature were set at $\theta_f = 300K$. The simulations aimed to understand and explore the combined impacts of the rotating cylinder on the heat convection and flow patterns when the buoyancy term is relevant.

Table 1: Summary of all numerical simulations performed for this work.

Reynolds	**Richardson**	α **(for IBM-VPM)**	α **(for OpenFOAM)**
40	0.5, 1.0, 1.5, 2.0	0, 1	0, 0.5, 1.0, 1.5, 2.0
100	0.5, 1.0, 1.5, 2.0	0, 1	0, 0.5, 1.0, 1.5, 2.0
150	0.5, 1.0, 1.5, 2.0	0, 1	0, 0.5, 1.0, 1.5, 2.0
200	0.5, 1.0, 1.5, 2.0	0, 1	0, 0.5, 1.0, 1.5, 2.0

3.1 Flow aspects

Figure 4 shows the pressure field for stationary cylinder with constant $Re = 100$ obtained by the OpenFOAM program. In Figure **(a)** are the results for $Ri = 0.5$ and **(b)** with $Ri = 1.5$. As noted by Bhattacharyya and Singh (2010), the imposition of heat on the cylinder surface increases the fluid velocity below it, as the fluid tend to move upwards. It is possible to observe that with a greater velocity field below the cylinder there should be a reduction on the pressure field at the region. This result can be seen as the buoyant term increases (and so that the amount of heat) from $Ri = 0.5$ to $Ri = 1.5$, from Fig. 4a to Fig. 4b, respectively.

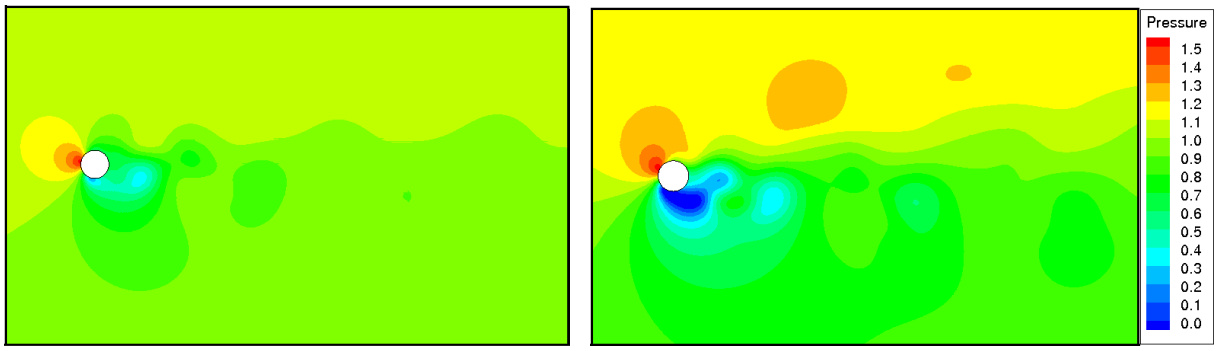

(a) (b)

Figure 4: Pressure fields for $Re = 100$. **(a)** $Ri = 0.5$. **(b)** $Ri = 1.5$. OpenFOAM.

Figure 5 shows the instantaneous vorticity contours for different values of Ri with constant $Re = 100$ and $\alpha = 0$. On the left column are shown the results obtained with OpenFOAM and on the right column the results from the program with the Immersed Boundary Method/Virtual Physical Method (called IBM-VPM) implemented. On the first row simulations were taken of with $Ri = 0.5$ and on the second row with $Ri = 1.5$. It is possible to note that for $Ri = 0.5$ the vortex shedding street still has a lengthwise patttern behaviour, as it occurs within a forced convective flow. With the increase of the buoyancy term significance (increase of Ri) the vortex shedding gains a little slop upwards and the vortex swirls increases its size.

The flow field asymmetry for cross flow configuration was already reported on literature by several authors (Kieft, Rindt and van Steenhoven, 2007; Bhattacharyya and Singh, 2010). As the fluid is heated on the cylinder neighborhood its density decreases and velocity increases by buoyancy effect. With a u non null incident velocity the result velocity magnitude makes the vortex shedding street incline.

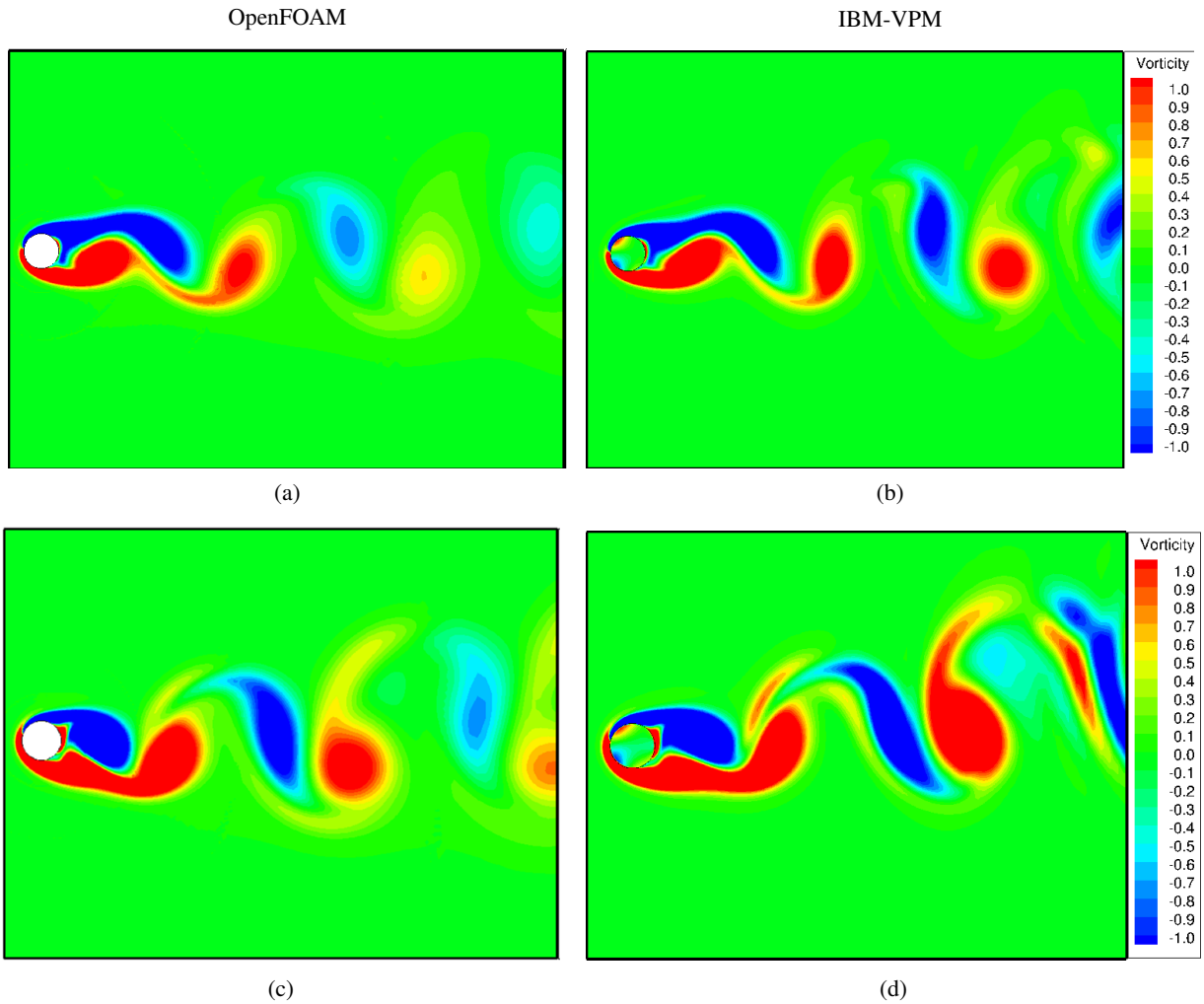

Figure 5: Vorticity fields for $Re = 100$ and $\alpha = 0$. Left side column, OpenFOAM. Right side column, IBM-VPM. For **(a)** and **(b)** $Ri = 0.5$, for **(c)** and **(d)** $Ri = 1.5$.

Figure 6 shows the effect of rotation of the cylinder associated with the buoyant term. All results were taken from the IBM-VPM cases with $Re = 100$. On the left column it is possible to see the velocity magnitude field for a stationary cylinder. On the right column the velocity magnitude for a rotating cylinder at $\alpha = 1$. On the first row, $Ri = 0.5$ and on the second one, $Ri = 1.5$. For cases with rotating cylinder, the counterclockwise movement ($\alpha > 0$) 'pushes in' the fluid in the same direction as the buoyancy term had already been moving it for stationary cases, i. e., from the bottom to the up side of the cylinder. Thus, cylinder rotation on the counterclockwise direction increses the fluid moviment tendency observed for a stationary cylinder subjected to an increase of the buoyant term. From Fig. 6a to 6d it is possible to note the increase on the total velocity magnitude, with the combined effect of rotation and buoyancy, with the increase of the scale grades.

3.2 Drag and Lift Coefficients and Strouhal Number

Figure 7 shows the drag coefficients for different combinations of Re, Ri and α. On Figure 7a is shown the drag coefficient *versus* Ri for different values of Re and on Fig. 7b is shown the drag coefficient *versus* α for $Re = 100$ varying the Ri number. It is possible to note a decrease on the drag absolute value with the increase of Ri. Also, a very pronunciated and almost linear decrease on drag with the increase of α. Paramane and Sharma (2010) detected the same reduction of drag coefficient with increase of Ri.

The drag coefficient is positive for stationary cylinder and becomes negative for rotating cylinder after certain α and Ri values indicating an inversion on the direction of drag force from forward to backward direction. Paramane and Sharma (2010) justified this decrease of drag coefficient for $Ri > 0$ and $\alpha > 0$ by the decreasing of the pressure and viscous drag force, for $Re = 40$ and $Re = 100$ with $0 \leq \alpha \leq 8$. The results of our simulations suggests that it occurs for Re up to 200 with $\alpha \leq 2$.

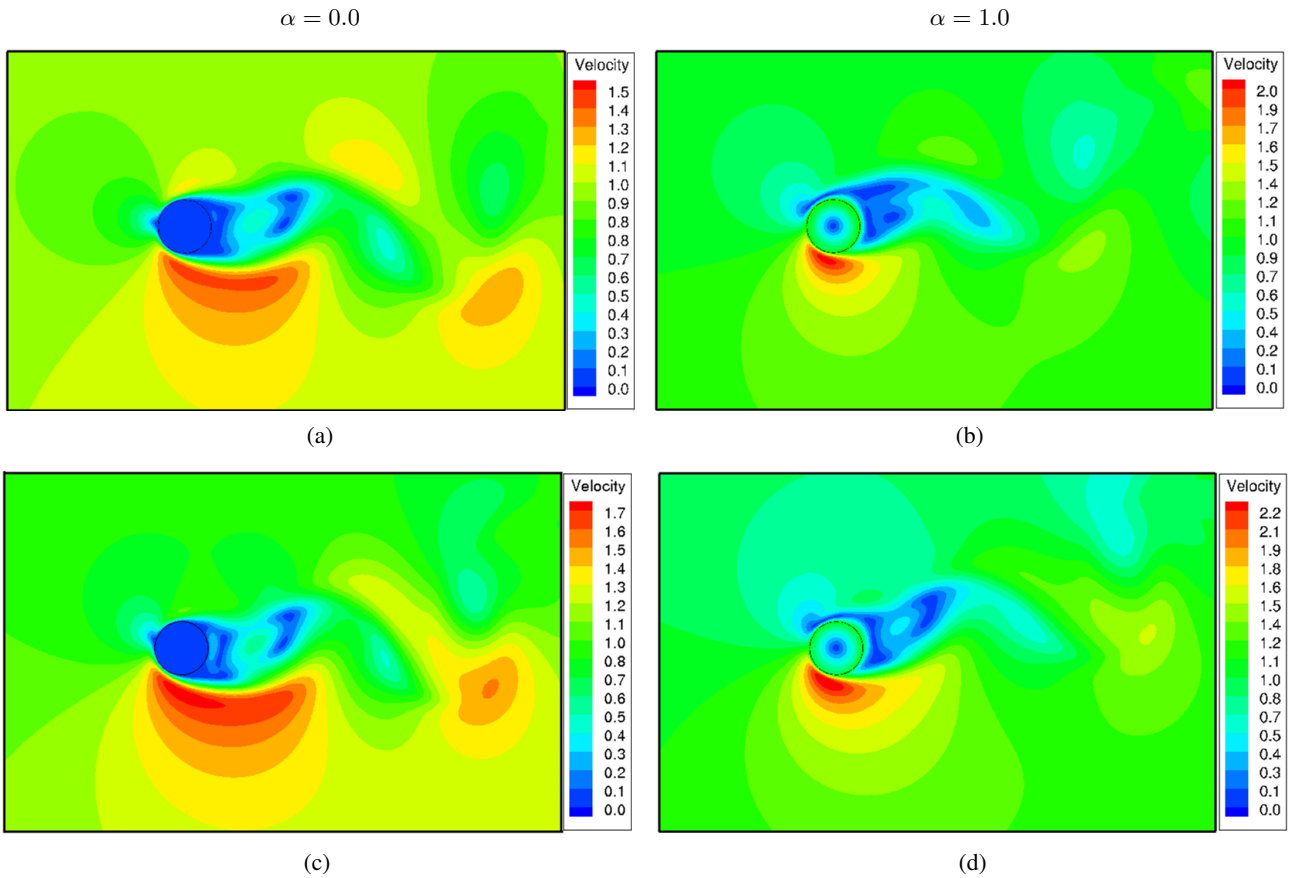

Figure 6: Velocity magnitude fields for $Re = 100$. Left side column, $\alpha = 0.0$. Right side column, $\alpha = 1.0$. For **(a)** and **(b)** $Ri = 0.5$, for **(c)** and **(d)** $Ri = 1.5$. IBM-VPM program.

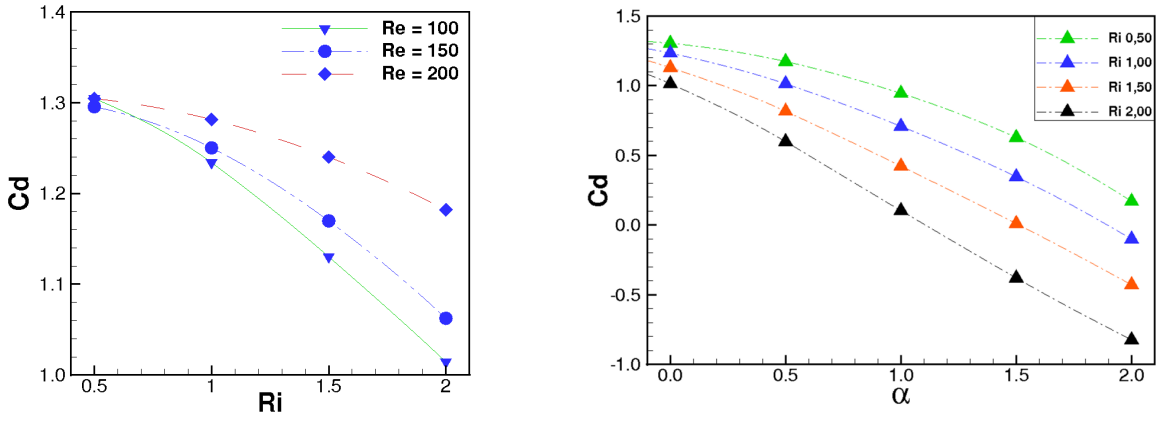

Figure 7: Drag coefficients: **(a)** for $\alpha = 0$ and different Ri and Re; **(b)** for $Re = 100$ and different Ri and α. OpenFOAM.

Figure 8a shows the lift coefficient *versus* Ri for different values of Re. The time-averaged lift coefficient is negative and increases almost linearly with the increase of cylinder temperature (increase of Ri) at a fixed Re. Kieft, Rindt and van Steenhoven (2007) and Bhattacharyya and Singh (2010) have also observed the same negative lift effect due to increase of Ri. As it had been seen in Fig. 4 the pressure above the cylinder is higher than the pressure below the cylinder when buoyancy effect is considered. This imbalance in the surface pressure due to the buoyancy produces a negative lift on the cylinder. Figure 8b shows the lift coefficient *versus* α for $Re = 100$. The combined effect of rotation and Ri increases the lift coefficient magnitude more drastically, as rotation acts at the same direction of fluid flow as Ri, as previous noted. Same results were found for other values of simulated Re and combined effects of α and Ri.

The periodic vortex shedding frequency is represented by Strouhal number, St, and it was determined from a Fast Fourier Transform (FFT) of temporal variation of lift coefficient. Its variation with increasing rotational velocity is shown in Fig. 9 for various α and Ri and $Re = 100$. The Strouhal number of stationary cylinder is almost equal to that of

cylinder rotating at $\alpha = 1$ and increases with increasing Ri for the stationary/rotating cylinder.

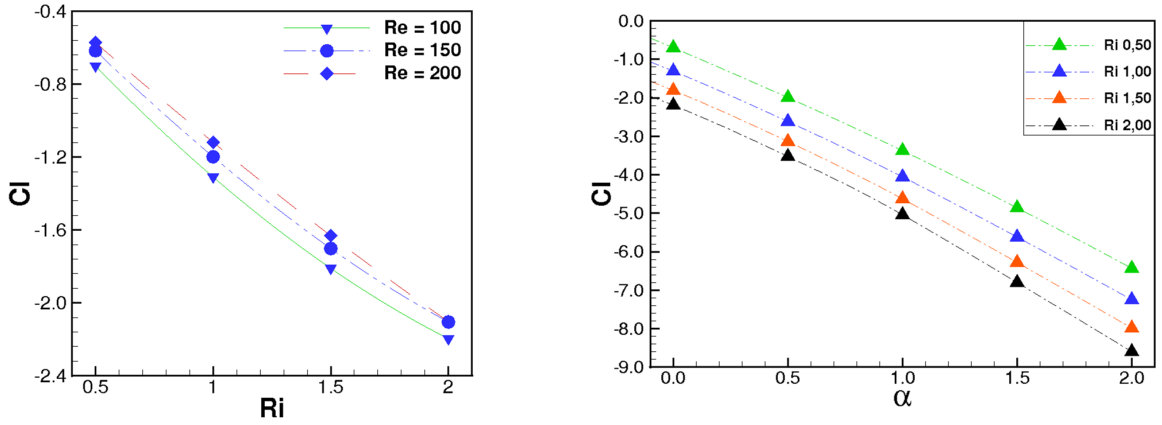

(a) (b)

Figure 8: Lift coefficients. **(a)** for $\alpha = 0$ and different Ri and Re; **(b)** for $Re = 100$ and different Ri and α. OpenFOAM.

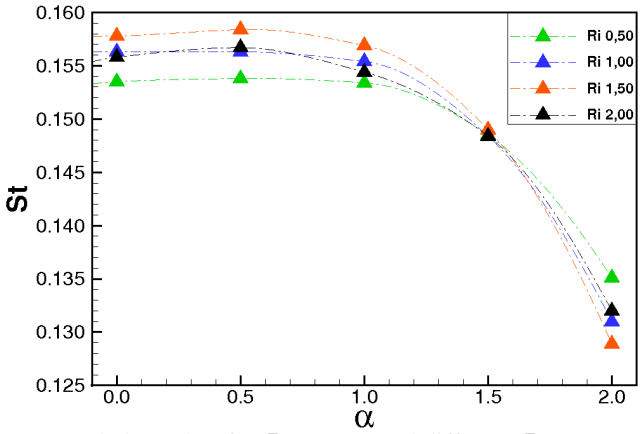

Figure 9: Strouhal number for $Re = 100$ and different Ri. OpenFOAM.

With the increase of heating on the cylinder surface (increase of Ri), the vortex formation is enhanced due to fluid acceleration with the gain of y velocity leading to faster movement of the vortices. With the increase in α, the Strouhal number drops sharply, which will ultimaly lead to vortex suppression, as demonstrated by Paramane and Sharma (2010), by the creation of an envelop layer of fluid around the cylinder.

3.3 Nusselt Number and numerical correlation

Time-averaged Nusselt number ($\overline{Nu}$) for $Re = 40$ and different Ri is shown on Tab. 2. OpenFOAM and IBM-VPM results can be directly compared, as they can be compared with literature. It was found that the rise of the Ri number produces a very small increment on the average rate of heat transfer, specially at small Re numbers ($Re = 40$). The response of $\overline{Nu}$ with the increase of Re is much faster than with the variation of Ri alone, as it can be observed on Fig. 10. The variation of $\overline{Nu}$ with Ri at a fixed Re is almost linear with a very mild slope. Thus, the convective heat transfer dominates in this range of Reynolds number ($Re \leq 200$).

Table 2: Time-averaged Nusselt number ($\overline{Nu}$) for $Re = 40$ and different Ri.

Ri	OpenFOAM	IBM-VPM	Badr (1982)	Chatterjee e Sinha (2016)
0,50	3,2726	3,0870	-	-
1,00	3,2524	3,1277	-	-
1,50	3,2047	3,1734	-	-
2,00	3,3147	3,2218	3,76	3,3972

Figure 11 shows that $\overline{Nu}$ decreases almost monotonically with the increase of α, for a constant $Re = 100$. Although not showed, as noted on Fig. 10, with the increase of Re there is a more significantly increase on the $\overline{Nu}$, but the overall

decreasing trend for greater values of α is equally observerd. Furthermore, the figure shows that $\overline{Nu}$ increases with the increase of Ri at a constant $\alpha > 0$, as observed for the stationary cylinder case.

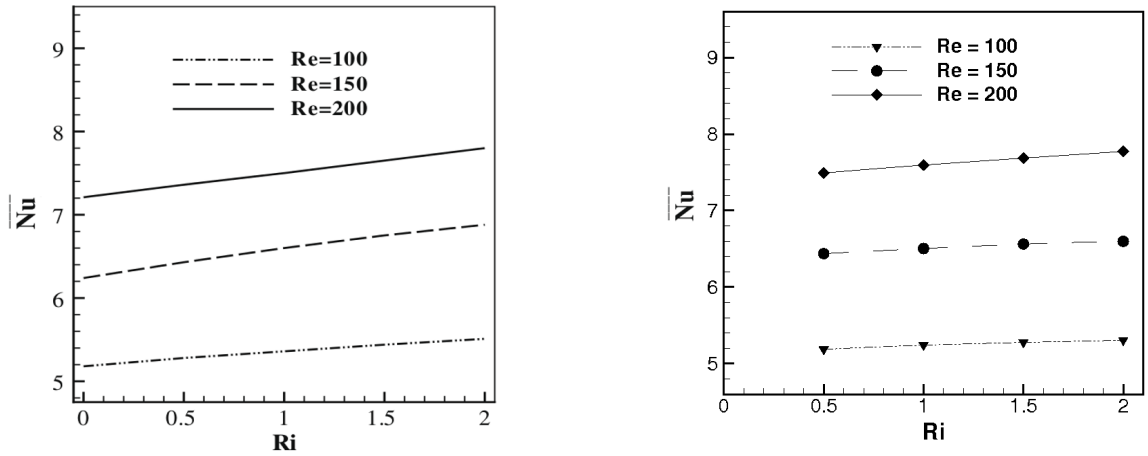

(a) (b)

Figure 10: Time-averaged Nusselt numbers for different Re and Ri with $\alpha = 0$. **(a)** Bhattacharyya and Singh (2010). **(b)** OpenFOAM.

The decrease of the time-averaged Nusselt number with the increase of α can be explained by the fluid envelop layer that rotation creates and which acts as a vortex suppresion and as a buffer zone for heat transfer between the cylinder and the fluid, restricting the heat transfer to conduction mainly. Furthermore, as demonstrated by Paramane and Sharma (2010), the size of enveloping vortex and its mean thickness increases with the increase of α resulting on a decrease of the thermal transfer.

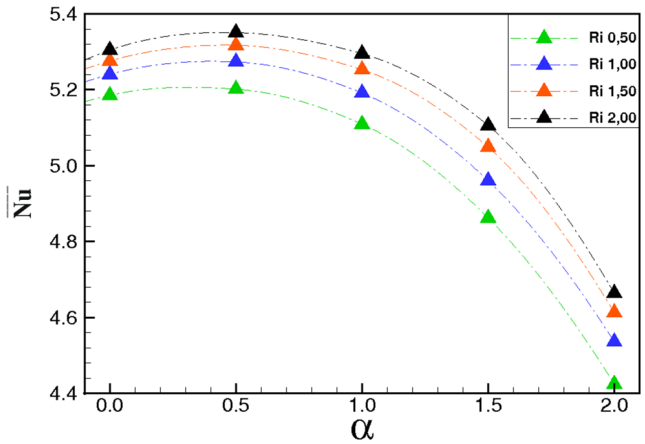

Figure 11: Time-averaged Nusselt numbers for different Ri and α with $Re = 100$. OpenFOAM.

From the obtained results, it is noticed that the influence of the absolute value of the rotation and the number of Reynolds are more predominant for $\overline{Nu}$ than Ri. In this way, only α and Re were used to create a correlation for the value of $\overline{Nu}$. The program used to create this correlation is called LABFit (Silva *et al.*, 2004). Consideration should be given to the linear growth of $\overline{Nu}$ with the increase of Re and the approximately parabolic format of $\overline{Nu}$ with the variation of α. Thus, for the same value of Re the curve should approach a parabola and, for the same value of α, the curve should behave linearly.

A function of α and Re for $\overline{Nu}$ prediction were generated by LABFit with the simulation points made with OpenFOAM. The correlation that best fit the numerical data has four parameters, A, B, C and D and can be written by:

$$\overline{Nu} = \frac{(A + B \cdot Re)}{1 + C \cdot \alpha + D \cdot \alpha^2} \tag{9}$$

being $A = 2.461$, $B = 0.02642$, $C = -0.03678$ e $D = -0.05828$.

Points used for adjustment include all simulated Ri values, althougt it was not used as a variable for the correlation adjustment. The resulting curve fit can be seen on Fig. 12 and is valid, with a confidence of 95%, for intervals of

$40 \leq Re \leq 200$, $0 \leq \alpha \leq 2$ and $0.5 \leq Ri \leq 2.0$. Residues from the adjustment are in the range of $-0.522 \leq R \leq 0.409$ with an average error of $1.027 \cdot 10^{-3}$.

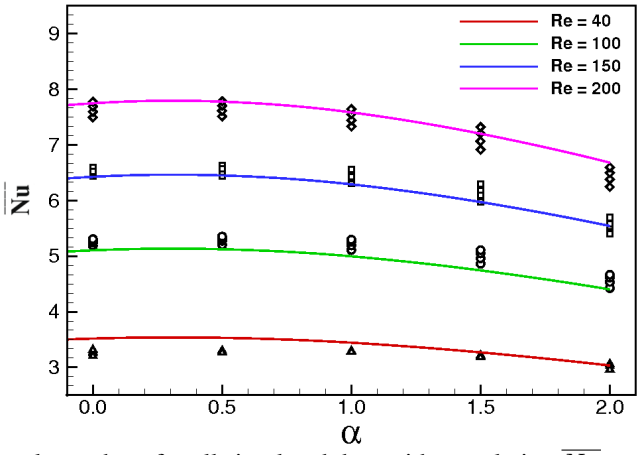

Figure 12: Time-averaged Nusselt numbers for all simulated data with correlation $\overline{Nu}$ *versus* α (Eq. 9) at different Re.

4. CONCLUSION

This paper presents a numerical study of the influence of buoyancy on a cross flow configuration over a stationary and rotating heated cylinder. Only a few papers consider all of these effects combined and their influence on the dimensionless parameters (Nusselt and Strouhal numbers, drag and lift coefficients). Two computational programs, based on different numerical methodologies, were used to perform the simulations.

Initially, stationary cylinder cases were studied with several Reynolds and Richardson number values (buoyancy parameter). For stationary cylinder the influence of the buoyancy term on the vortex street and on heat transfer was investigated. For the Reynolds number values investigated it was noted that the heating process increases vortex formation and detachment as well as decreases the aerodynamics coefficients due to an increase on the field magnitude velocities.

Then, rotation around the cylinder own axis was imposed at various specific values (α). With the rotating cylinder it was verified that even with the greater Richardson numbers the rotation becomes a more significant parameter than the heating to characterize the flow. At a fixed value of rotation, the variation of Ri becomes less significant. Counterclockwise rotation acts as a suppressor of the vortex and heat transfer, as is creates a buffer envelop layer around the cylinder, which also reduces drastically the drag and lift coefficients.

An empirical correlation was also proposed for the Nusselt number as a function of Re and α using the results obtained with the OpenFOAM code. This correlation can be used for the ranges $40 \leq Re \leq 200$, $-2 \leq \alpha \leq 2$ and $0.5 \leq Ri \leq 2.0$ and it did not take into account variation on Ri.

As a suggestion for future work, the following topics are proposed: to simulate larger values of rotation, both clockwise and counterclockwise to investigate the change in flow direction; perform simulations with other Prandtl number values and study it influence associated with buoyancy and cylinder rotation; to perform a larger number of simulations to propose a correlation that includes higher Reynolds number values and other rotation values.

5. ACKNOWLEDGEMENTS

The authors would like to thank CAPES for the scholarship and CNPq and FAPEMIG (TEC-APQ-00893-17) for the financial support.

This work has made use of the computing facilities available at the Laboratory of Computational Astrophysics of the Universidade Federal de Itajubá (LAC-UNIFEI). The LAC-UNIFEI is maintained with grants from CAPES, CNPq and FAPEMIG.

6. REFERENCES

Badr, H., 1983. "A theoretical study of laminar mixed convection from a horizontal cylinder in a cross stream". *International Journal of Heat and Mass Transfer*, Vol. 26, No. 5, pp. 639 – 653. ISSN 0017-9310.

Bhattacharyya, S. and Singh, A., 2010. "Vortex shedding and heat transfer dependence on effective reynolds number for mixed convection around a cylinder in cross flow". *International Journal of Heat and Mass Transfer*, Vol. 53, No. 15–16, pp. 3202 – 3212. ISSN 0017-9310.

Chatterjee, D. and Sinha, C., 2016. "Effect of prandtl number and rotation on vortex shedding behind a circular cylin-

der subjected to cross buoyancy at subcritical reynolds number". *International Communications in Heat and Mass Transfer*, Vol. 70, pp. 1 – 8. ISSN 0735-1933.

Kieft, R., Rindt, C. and van Steenhoven, A., 2007. "Near-wake effects of a heat input on the vortex-shedding mechanism". *International Journal of Heat and Fluid Flow*, Vol. 28, No. 5, pp. 938 – 947. ISSN 0142-727X.

Lima E Silva, A., 2002. *Desenvolvimento e Implementação de uma nova Metodologia para Modelagem de Escoamentos sobre Geometrias Complexas: Método da Fronteira Imersa com Modelo Físico Virtual*. Ph.D. thesis, Universidade Federal de Uberlândia. Tese de Doutorado.

Lima E Silva, A., Silveira-Neto, A. and Damasceno, J.J.R., 2003. "Numerical simulation of two-dimensional flows over a circular cylinder using the immersed boundary method". *J. Comput. Phys.*, Vol. 189, No. 2, pp. 351–370. ISSN 0021-9991.

Lima E Silva, A.L.F., Silva, A.R. and Silveira-Neto, A., 2007. "Numerical simulation of two-dimensional complex flows around bluff bodies using the immersed boundary method". *Journal of the Brazilian Society of Mechanical Sciences and Engineering*, Vol. 29, pp. 379 – 387. ISSN 1678-5878.

Lima E Silva, A.L.F.d. and Lima E Silva, S.M.M., 2007. "Numerical simulation of flows over cylinders under the influence of buoyancy using the immersed boundary method". *19th International Congress of Mechanical Engineering*.

Oliveira, J.E.S., Lima E Silva, A.L.F.d. and Silveira-Neto, A.d., 2006. "Influência de modelos de turbulência na simulação de escoamentos sobre aerofólios móveis usando o método de fronteira imersa". Technical report, IV Congresso Nacional de Engenharia Mecânica.

Paramane, S.B. and Sharma, A., 2010. "Effect of cross-stream buoyancy and rotation on the free-stream flow and heat transfer across a cylinder". *International Journal of Thermal Sciences*, Vol. 49, No. 10, pp. 2008 – 2025. ISSN 1290-0729.

Santos, R.D.C.D., 2014. "Análise bidimensional termo-fluido dinâmica de cilindros rotativos com o método da fronteira imersa / modelo físico virtual". Dissertação de Mestrado.

Silva, W.P.d., Silva, C.M.e., Cavalcanti, C.G., Silva, D.D.e., Soares, I.B., Oliveira, J.A. and Silva, C.D.e., 2004. "LAB Fit ajuste de curvas: um software em portugues para tratamento de dados experimentais". *Revista Brasileira de Ensino de Fisica*, Vol. 26, pp. 419 – 427. ISSN 1806-1117.

Vilaça, A.C., Lima E Silva, A.L.F.d. and Silveira-Neto, A.d., 2004. "Modelagem matemática e simulação numérica do escoamento sobre uma partícula em queda livre". Technical report, XXXI ENEMP - Congresso Brasileiro de Sistemas Particulados.

7. RESPONSIBILITY NOTICE

The authors are the only responsible for the printed material included in this paper.